




Human Embryonic Stem Cell-Derived Oligodendrocyte Progenitor Cells: Preclinical Efficacy and Safety in Cervical Spinal Cord Injury

NATHAN C. MANLEY ^{a,*} CATHERINE A. PRIEST,^{b,*} JERROD DENHAM,^b EDWARD D. WIRTH III,^{a,b}
JANE S. LEBKOWSKI^{a,b}

Key Words. Cervical spinal cord injury • Spinal cord injury • Preclinical • Oligodendrocyte progenitor cell • Human embryonic stem cell • Clinical trial

^aAsterias Biotherapeutics Inc., Dumbarton Circle, Fremont, California, USA;
^bGeron Corporation, Menlo Park, California, USA

*Contributed equally.

Correspondence: Nathan C. Manley, Ph.D., Asterias Biotherapeutics Inc., 6300 Dumbarton Circle, Fremont, California 94555, USA.
Telephone: 510-456-3820, Fax: 510-456-3796, e-mail: nmanley@asteriasbio.com

Received March 20, 2017; accepted for publication July 24, 2017; first published August 22, 2017.

<http://dx.doi.org/10.1002/sctm.17-0065>

This is an open access article under the terms of the Creative Commons Attribution-NonCommercial-NoDerivs License, which permits use and distribution in any medium, provided the original work is properly cited, the use is non-commercial and no modifications or adaptations are made.

ABSTRACT

Cervical spinal cord injury (SCI) remains an important research focus for regenerative medicine given the potential for severe functional deficits and the current lack of treatment options to augment neurological recovery. We recently reported the preclinical safety data of a human embryonic cell-derived oligodendrocyte progenitor cell (OPC) therapy that supported initiation of a phase I clinical trial for patients with sensorimotor complete thoracic SCI. To support the clinical use of this OPC therapy for cervical injuries, we conducted preclinical efficacy and safety testing of the OPCs in a nude rat model of cervical SCI. Using the automated TreadScan system to track motor behavioral recovery, we found that OPCs significantly improved locomotor performance when administered directly into the cervical spinal cord 1 week after injury, and that this functional improvement was associated with reduced parenchymal cavitation and increased sparing of myelinated axons within the injury site. Based on large scale biodistribution and toxicology studies, we show that OPC migration is limited to the spinal cord and brainstem and did not cause any adverse clinical observations, toxicities, allodynia, or tumors. In combination with previously published efficacy and safety data, the results presented here supported initiation of a phase I/IIa clinical trial in the U.S. for patients with sensorimotor complete cervical SCI. *STEM CELLS TRANSLATIONAL MEDICINE* 2017;6:1917–1929

SIGNIFICANCE STATEMENT

In this article, we provide a detailed account of the preclinical animal studies that demonstrated efficacy and safety of an oligodendrocyte progenitor cell therapy product currently in clinical testing in the U.S. for patients with cervical spinal cord injury (SCiStar clinical trial). Disclosure of this work is important not only because it documents the supporting data that led to initiation of the SCiStar clinical trial, but also because it provides examples of the kinds of preclinical testing that should be considered for future pluripotent stem cell-based therapies that target neurological injury and disease.

INTRODUCTION

The pathophysiology associated with spinal cord injury (SCI) involves a complex cascade of events including edema, hemorrhage, inflammation, severing of axons, parenchymal cavitation, and loss of myelin-producing oligodendrocytes [1–4]. The clinical outcome of SCI typically involves severe functional impairment, including limb paralysis, aberrant pain signaling, and loss of bladder and sexual function [5]. Given the complex milieu of cellular events that underlie these functional impairments, effective treatment of SCI likely will require combinatorial approaches or therapies with multiple mechanisms of action.

AST-OPC1 (formerly GRNOPC1) is a cell therapy product comprised of oligodendrocyte progenitors (OPCs) that was originally differentiated from the H7 human embryonic stem cell (hESC) line [6]. Subsequent to early preclinical studies, AST-OPC1 has been produced from the H1 hESC line for all preclinical testing and clinical development. AST-OPC1 expresses early stage OPC markers, such as nestin, neural/glial antigen 2 (NG2/CSPG4), and platelet derived growth factor receptor alpha [7], and is produced by a commercially scalable process that has been independently replicated by multiple groups [8]. In vitro and in animal models, AST-OPC1 has exhibited several activities relevant to central nervous

system (CNS) repair, including neurotrophic factor secretion [9, 10], stimulation of axon outgrowth [6], suppression of parenchymal cavitation [10, 11], maturation into myelin producing oligodendrocytes [6, 10], and enhancement of motor behavioral recovery post-SCI [11, 12].

We recently reported the preclinical safety testing of AST-OPC1 in thoracic SCI [10], which, in conjunction with efficacy testing [6, 11], led to initiation of a phase I clinical trial for patients with sensorimotor complete thoracic SCI. Initial testing of AST-OPC1 in thoracic SCI was based on a more favorable risk/benefit assessment relative to cervical SCI, including animal safety data that confirmed a minimal risk of administered cells migrating to the brain and causing potential unwanted side effects. Concurrent with the initiation of clinical testing of AST-OPC1 in thoracic SCI, preclinical studies exploring the efficacy and safety of AST-OPC1 administration into the cervical spinal cord were conducted.

Development of AST-OPC1 as a treatment for cervical SCI was based on multiple considerations. Relative to thoracic SCI, which accounts for approximately 35% of clinical SCI cases in the U.S., the majority of SCI cases (54%) occur at the cervical level, affecting over 9,000 individuals annually (NSCISC. 2016 Facts and Figures at a Glance). Because the functional deficits associated with cervical SCI typically involve the arms and hands, rehabilitative therapies largely focus on regaining motor skills in the arms, fingers, and hands [5], thus providing more defined efficacy endpoints that can substantially improve quality of life. Finally, a cervical lesion is potentially more conducive to regeneration given that affected white matter is closer to the neuronal cell bodies of origin, and subsequent axonal outgrowth could be stimulated by AST-OPC1 secretion of neurotrophic factors such as midline [9, 13].

Here we report the efficacy and safety testing of AST-OPC1 in a nude rat model of cervical SCI. For these studies, we used a previously established unilateral contusion injury model [14–18] to allow assessment of AST-OPC1 in the context of a white matter lesion and with resulting motor behavioral deficits predominantly restricted to the ipsilateral forelimb, thus providing within-subject controls (i.e., the contralateral forelimb) and tracking of behavioral recovery that is potentially meaningful to patient outcome [5]. To assess efficacy, motor behavioral recovery was measured using the TreadScan system followed by histological examination of the injury/graft site. To assess safety, we performed biodistribution and toxicology studies in accordance with current Good Laboratory Practices (cGLP), examining AST-OPC1 engraftment and migration within the CNS and whether any unwanted side effects were detected.

Together the efficacy and safety data reported here were submitted to the U.S. Food and Drug Administration (FDA) as part of an Investigational New Drug (IND) amendment for AST-OPC1, proposing its advancement in clinical testing to cervical SCI. Based on these results, in combination with previously published preclinical efficacy and safety data [6, 10–12], and a favorable safety profile obtained from the AST-OPC1 thoracic SCI clinical trial [19], a phase I/IIa clinical trial sponsored by Asterias Biotherapeutics was initiated in the U.S. in 2014, testing the direct intraspinal cord administration of AST-OPC1 in patients with sensorimotor complete cervical SCI.

MATERIALS AND METHODS

Please see the Supporting Information Materials and Methods for additional methodology details.

Animal Subjects

All procedures used in this study were approved by a board-certified veterinarian and the Geron IACUC committee and were conducted in accordance with the National Institute of Health Guide for the Care and Use of Laboratory Animals. Adult athymic nude rats (strain Crl:NIH-Foxn1^{tmu}) were used for all studies.

Differentiation of AST-OPC1 From hESCs

The WA01 (H1) hESC line was expanded in feeder-free conditions [20, 21] and differentiated into AST-OPC1 according to published methods [10] and as described in the Supporting Information Materials and Methods. All studies were performed using cryopreserved and thawed AST-OPC1 cells, in accordance with their use in the subsequent cervical SCI clinical trial.

Cervical SCI

Adult female nude rats were subjected to a unilateral cervical spinal cord contusion injury at level C5 using the Infinite Horizons Impactor (Precision Systems & Instrumentation, Fairfax, VA, www.presysin.com) set at a force impact of 250 kilodynes for efficacy testing (severe injury) or 150 kilodynes for biodistribution and toxicology testing (moderate injury), as described previously [22] and in the Supporting Information Materials and Methods.

AST-OPC1 Transplantation in Injured Nude Rats

One week (7 ± 1 day) after cervical SCI, AST-OPC1 at 2.4×10^5 cells per rat (efficacy dose, 2.4 μ l single injection) or 2.4×10^6 cells per rat (maximum feasible dose, 4 \times 6 μ l injections) or equivalent volumes of vehicle (Hanks' Balanced Salt Solution, HBSS) was injected directly into the spinal cord parenchyma adjacent to the injury site using a Hamilton microsyringe and stereotaxic frame. Additional details and rationale for the transplantation strategy are provided in the Supporting Information Materials and Methods.

Assessment of Locomotor Performance with the TreadScan System

Prior to injury, and at 1, 2, and 4 months post-transplantation of AST-OPC1 or vehicle, rats were assessed for locomotor function using the TreadScan system (Clever Sys, Inc., Reston, VA, clever-sys.com) according to the manufacturer's guidelines and as described in the Supporting Information Materials and Methods and Supporting Information Table 1.

Animal Perfusion and Histology

Spinal cord and brain tissues were collected at autopsy and processed by formalin fixation and paraffin-embedding for subsequent hematoxylin and eosin (H&E) staining, in situ hybridization (ISH), and immunohistochemistry (IHC). To identify myelinated fibers within the spinal cord, tissues were stained with Eriochrome cyanine (EC) solution and counterstained with Eosin-Y. All animals that received AST-OPC1 transplantation were assayed for the presence of human cells in the spinal cord by ISH with a human ALU (hALU) DNA repeat sequence probe (Cat. # Q151P.9900, Thermo Fisher Scientific, Waltham, MA, <http://www.thermofisher.com>). Parallel tissue sections were stained by IHC for Ki67 (Cat. # ab833, Abcam, Cambridge, MA, <http://www.abcam.com>) using standard methodology.

Cavitation Area Measurements in the Injured Spinal Cord

Measurements of maximal cavitation area were performed on EC-stained spinal cord tissue sections by an investigator who was blinded to the treatment groups. For each animal, all longitudinal cervical spinal cord tissue sections containing the injury site were assessed, and the tissue section containing the maximal lesion area was quantified using ImageJ software (NIH, Bethesda, MD) and JMP 11 (SAS, Cary, NC, <http://www.jmp.com>).

Biodistribution of Transplanted AST-OPC1 by Histology and Quantitative PCR

For both biodistribution studies, adult female nude rats were subjected to cervical SCI and transplantation surgeries as described above, and tissues were then assessed histologically by ISH or by PCR at 2 days, and 3, 6, and 9 months post-transplant.

Clinical and Toxicological Assessments of AST-OPC1-Treated, Contused Rats

Toxicology studies of AST-OPC1-treated, female athymic nude rats were performed at MPI Research (Mattawan, MI, <http://www.mpiresearch.com>) in accordance with cGLP. In-life observations were conducted for 9 months followed by full necropsy and histopathology evaluations of spinal cord and brain by a board-certified veterinary pathologist who was blinded to the treatment groups.

Allodynia Measurements in AST-OPC1-Treated, Contused Rats

As part of one toxicology study, at both 4 and 8 months post-transplantation, subjects were evaluated for allodynia or hypersensitivity in response to normally non-noxious warm or cold stimuli [23].

RESULTS

Efficacy of AST-OPC1 in the Nude Rat Cervical SCI Model

To measure motor behavioral recovery after cervical SCI, we performed automated gait analysis using the TreadScan system prior to injury and monthly until 4 months post-treatment. A total of 90 parameters of locomotor and gait performance was measured by TreadScan and used to track motor behavioral recovery after injury and administration of 2.4×10^5 AST-OPC1 cells per rat, hereafter referred to as the AST-OPC1 efficacy dose. Descriptions of the individual TreadScan parameters are shown in Supporting Information Table 1. To calculate an overall gait score and recovery rate for each animal, a first principal component analysis (PCA) was performed to summarize the 90 measures into a single value and plotted over time (Fig. 1A). Relative to uninjured (Sham) animals, animals subjected to cervical SCI exhibited a reduced gait score at 1 month irrespective of treatment. However, beginning at 2 months and increasing at 4 months, animals administered AST-OPC1 exhibited an improving gait score more closely matched to that of the Sham group, whereas those treated with HBSS showed little recovery ($p = .045$, mixed linear effect model; Sham, $N = 8$; HBSS, $N = 16$; AST-OPC1, $N = 16$). When compared to animals treated with vehicle, animals treated with AST-OPC1 also exhibited improved performance in individual TreadScan measures; parameters that exhibited the greatest improvement in the AST-OPC1 group relative to the vehicle group were average running speed,

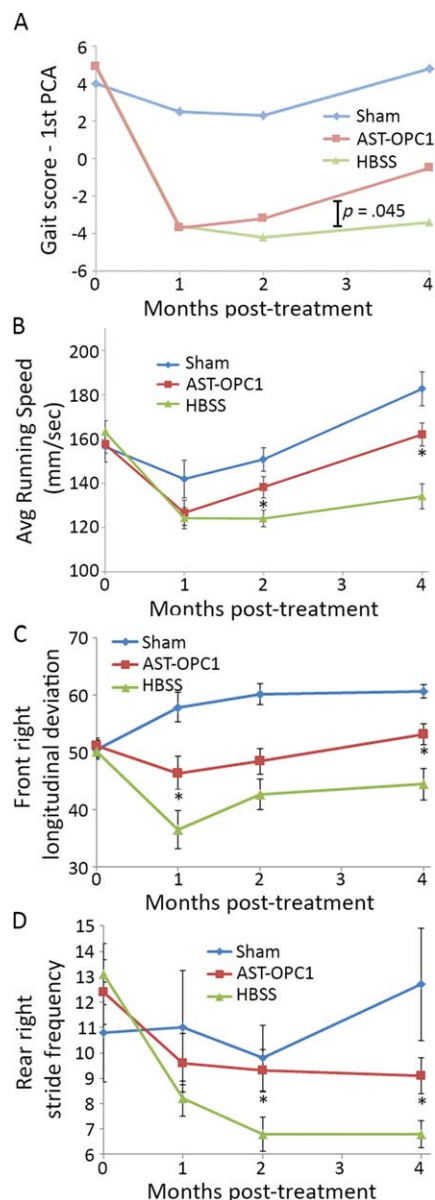


Figure 1. AST-OPC1 promotes motor behavioral recovery after cervical spinal cord injury (SCI). Animals were assessed for locomotor performance on the TreadScan system after sham surgery (laminectomy only) or cervical SCI and administration of vehicle (HBSS) or 2.4×10^5 AST-OPC1 cells. **(A):** The first PCA of all 90 TreadScan parameters was used to determine an overall gait score for each animal, and treatment group means are plotted versus time. After the first month post-treatment, animals treated with AST-OPC1 exhibited improvements in their gait score more closely matched to the Sham group, while animals treated with HBSS alone exhibited minimal improvements ($p = .045$, mixed linear model). **(B–D):** The top three individual TreadScan parameters indicating a significant improvement of AST-OPC1 treatment relative to vehicle treatment, including: (B) average running speed; (C) average front right maximal longitudinal deviation, which measures the greatest distance of the front paw from midline on the injured right side; (D) average rear right stride frequency, which measures the number of strides per second for the rear paw on the injured side. Asterisks denote a significant difference between the AST-OPC1 and HBSS treatment groups as determined by two-tailed Student's *t* test ($p < .05$). Error bars denote standard error of the mean (SEM). Sample sizes were as follows, Sham, $N = 8$; HBSS, $N = 16$; AST-OPC1, $N = 16$. Abbreviations: HBSS, Hanks' balanced salt solution; PCA, principal component analysis.

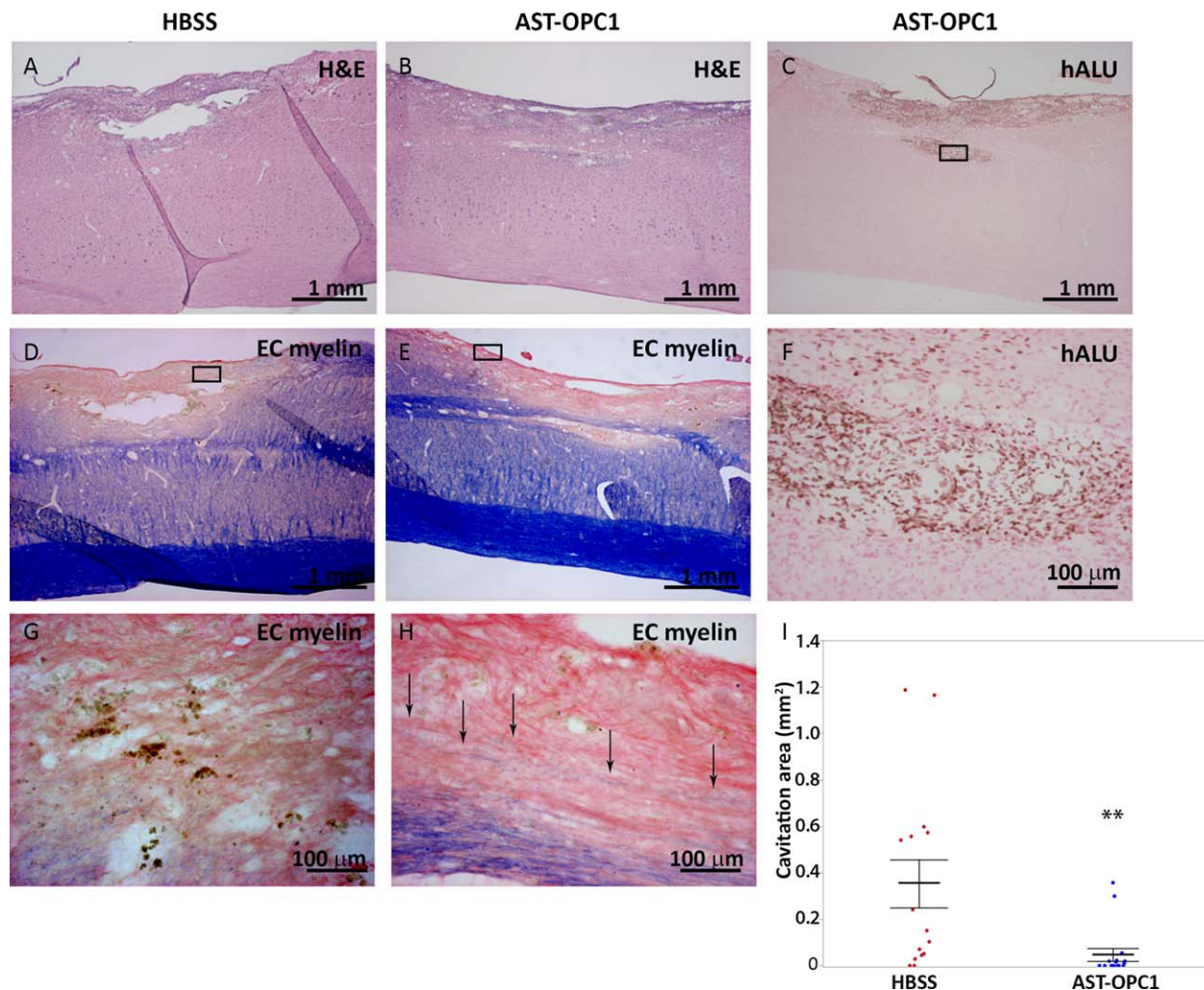


Figure 2. AST-OPC1 administration results in engraftment, reduced cavitation and increased myelination within the injury site at 4 months after cervical spinal cord injury. Representative photomicrographs of the cervical contusion injury site for rats treated with HBSS or 2.4×10^5 AST-OPC1 cells. (A, B): Spinal cord tissue sections from an HBSS- (A) or AST-OPC1- (B) treated rat stained with H&E to show overall pathology of the lesion site. (C): In situ hybridization-based labeling of the injury/graft site of an AST-OPC1-treated rat using a hALU DNA repeat element probe shows the presence of surviving human cells (brown nuclear label, surrounding tissue counterstained with eosin). Black box indicates the region shown at higher magnification in panel (F). (D, E): Histological labeling of myelin by EC myelin (counterstained with eosin) within the injury/engraftment site and surrounding tissue in an HBSS- (D) or AST-OPC1- (E) treated rat. Black boxes in (D) and (E) indicate the regions shown at higher magnification in panels (G) and (H), respectively. Black arrows in (H) indicate EC myelin-positive fibers within the lesion site of an AST-OPC1-treated rat. (I): Dot plot of parenchymal cavitation area for HBSS- (red dots) and AST-OPC1- (blue dots) treated rats 4 months post-injury/treatment. Treatment group means are indicated by the central horizontal lines, and error bars denote SEM. Asterisks denotes significance of AST-OPC1 treatment relative to HBSS by Student's *t* test ($p = .0069$). Sample sizes: HBSS, $N = 16$; AST-OPC1, $N = 16$. Abbreviations: EC, eriochrome cyanine; H&E, hematoxylin and eosin; HBSS, Hanks' balanced salt solution; hALU, human ALU.

front right longitudinal deviation, and rear right stride frequency (Fig. 1B–1D).

At 4 months post-injury/treatment, spinal cords were examined histologically to assess the injury site and extent of AST-OPC1 engraftment. Compared to HBSS, AST-OPC1 treatment resulted in a significant reduction in parenchymal cavitation at the injury site, with many AST-OPC1-treated animals showing little to no cavitation (Fig. 2A, 2B). Using ISH-labeling of hALU, robust AST-OPC1 engraftment was observed within and around the injury site (Fig. 2C, 2F), with comparable levels of engraftment observed in 16 of 16 assessed animals. In addition, while HBSS-treated animals typically exhibited no myelinated axons within the injury site (often due to the presence of a large cavity), eriochrome cyanine-labeled myelinated axons were observed within the injury site following

AST-OPC1 treatment (Fig. 2D, 2E, 2G, 2H). Quantification of maximal cavitation area within the lesion site indicated significant cavity reduction with AST-OPC1 relative to HBSS treatment (Fig. 2I, $p = .0069$, Student's *t* test).

Biodistribution of AST-OPC1 in the Nude Rat Cervical SCI Model

Two biodistribution studies were conducted in nude rats subjected to cervical SCI and assessed the AST-OPC1 efficacy dose (2.4×10^5 cells per rat, see Figs. (1 and 2)) and the maximum feasible dose of AST-OPC1 (2.4×10^6 cells per rat, maximum based on volume constraints of the cervical spinal cord). Because prior thoracic SCI biodistribution studies confirmed the absence of AST-OPC1 in peripheral tissues [10], the present analyses were limited

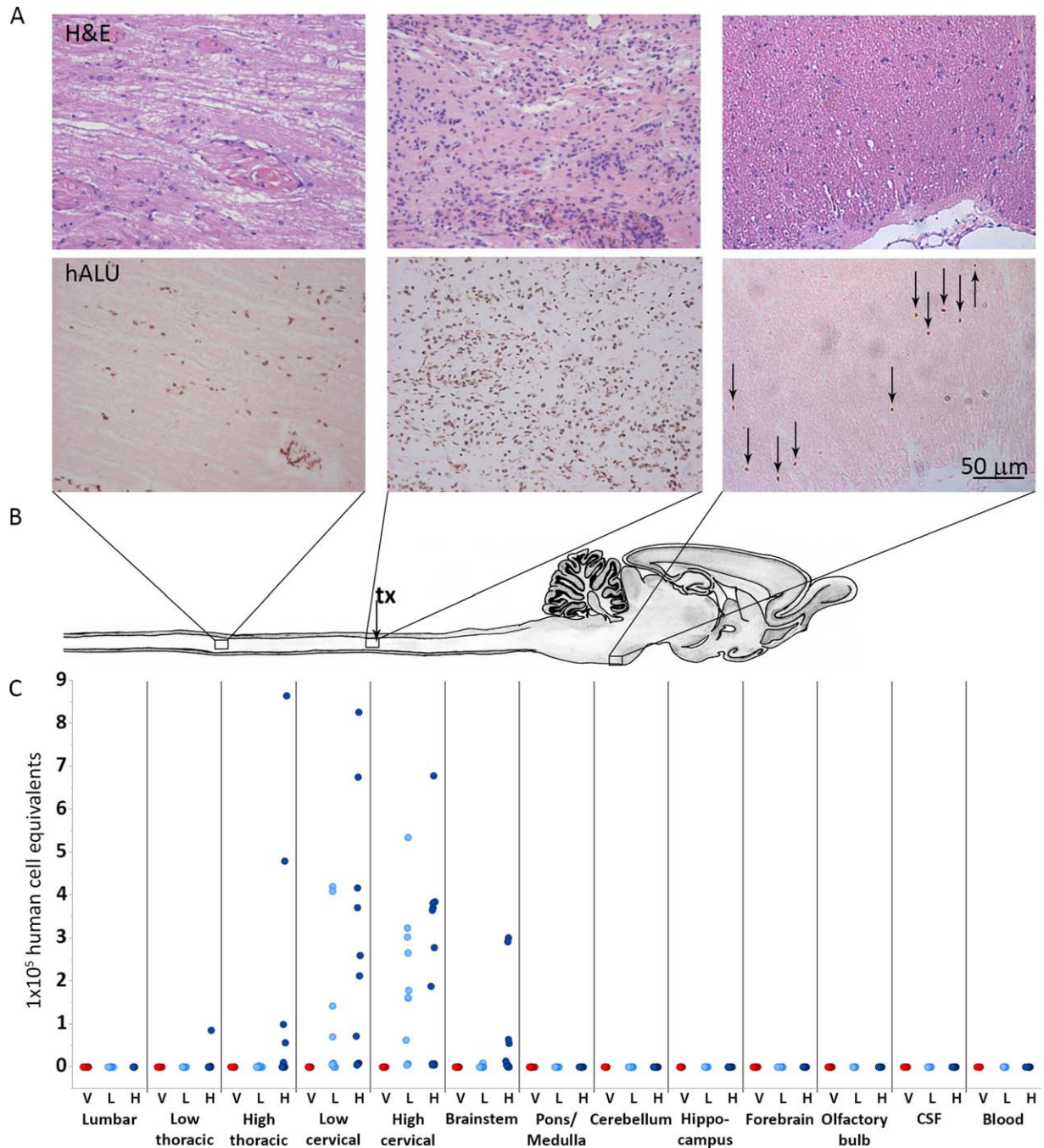


Figure 3. AST-OPC1 administration into the injured cervical spinal cord results in biodistribution that is limited to the spinal cord and brainstem. **(A):** Representative photomicrographs from rats treated with high dose AST-OPC1 and assessed histologically at 9 months post-treatment. The top panels in Figure 3A show representative H&E staining, and the bottom panels of Figure 3A show representative hALU staining of the most caudal distribution of cells positive for hALU (T1-T2 thoracic spinal cord, left panels), the highest density of hALU positive cells observed within the cervical injury/AST-OPC1 transplant site (middle panels), and the most rostral distribution of hALU positive cells (brainstem, caudal to pontine nucleus, right panels) observed with high dose AST-OPC1 treatment. **(B):** Schematic of rat spinal cord and brain indicating regions of representative photomicrographs shown in (A) and aligned with biodistribution dot plot shown in (C). The cervical injury/AST-OPC1 transplant site is indicated (tx, black arrow). **(C):** Dot plot of AST-OPC1 biodistribution at 6 months post-administration into the injured cervical spinal cord as determined by quantitative real-time PCR for hALU. Consistent with the histology shown in (A), quantitation of hALU by PCR indicated the highest density of human cells in the cervical spinal cord, and the most rostral and caudal migration of human cells extending to the brainstem and thoracic spinal cord (high dose AST-OPC1 only), respectively. Abbreviations: CSF, cerebral spinal fluid; H, high dose AST-OPC1 (2.4×10^6 cells per rat); hALU, human ALU; H&E, hematoxylin and eosin; L, low dose AST-OPC1 (2.4×10^5 cells per rat); V, vehicle.

to the CNS, cerebral spinal fluid (CSF), and blood. In one study, conducted in accordance with cGLP, animals were assessed clinically until 2 days (HBSS, $N = 10$; 2.4×10^5 AST-OPC1, $N = 10$;

2.4×10^6 AST-OPC1, $N = 10$), 3 months (HBSS, $N = 10$; 2.4×10^5 AST-OPC1, $N = 13$; 2.4×10^6 AST-OPC1, $N = 18$), 6 months (HBSS, $N = 9$; 2.4×10^5 AST-OPC1, $N = 13$; 2.4×10^6 AST-OPC1,

$N = 18$), or 9 months (HBSS, $N = 5$; 2.4×10^5 AST-OPC1, $N = 9$; 2.4×10^6 AST-OPC1, $N = 20$) post-treatment, followed by histological examination of the spinal cord and brain for surviving human cells by detection of hALU by ISH. In a second study, CNS tissues, CSF, and blood were collected at 2 days (HBSS, $N = 10$; 2.4×10^5 AST-OPC1, $N = 10$; 2.4×10^6 AST-OPC1, $N = 10$), 3 months (HBSS, $N = 11$; 2.4×10^5 AST-OPC1, $N = 11$; 2.4×10^6 AST-OPC1, $N = 11$), or 6 months (HBSS, $N = 11$; 2.4×10^5 AST-OPC1, $N = 11$; 2.4×10^6 AST-OPC1, $N = 11$) post-treatment and quantitatively assessed for hALU by PCR. AST-OPC1 biodistribution was assessed during the subacute phase post-SCI (9 days, 2 days post-transplant) defined by ongoing tissue remodeling and increased blood-spinal cord barrier permeability at the injury site, and during the chronic phase post-SCI (3, 6, 9 months) when tissue remodeling typically is resolved and the blood-spinal cord barrier integrity has re-established [24–26].

Histological examination of AST-OPC1 biodistribution indicated a similar engraftment and migration profile as seen previously for thoracic SCI [10]. Visualization of surviving AST-OPC1 cells by ISH indicated robust survival at all time points in 111 of 112 assessed animals, with the highest density of surviving cells present in the cervical spinal cord within and around the injury site (Fig. 3A, central panels). At 9 months, AST-OPC1 migration extended approximately 5 cm rostrally/caudally along the spinal cord. When the maximum feasible dose of AST-OPC1 was administered (2.4×10^6 cells per rat), AST-OPC1 cells were detected rostrally as far as the pyramidal tract in the pons, caudal of the pontine nucleus (Fig. 3A, right panels) and at a maximum caudal location of levels T1-T2 of the thoracic spinal cord (Fig. 3A, left panels). In contrast, administration of the efficacy dose of AST-OPC1 (2.4×10^5 cells per rat) resulted in migration that was restricted to the cervical spinal cord. Besides the small number of cells observed in the brainstem/pons, no AST-OPC1 cells were detected in any other brain regions.

Quantification of hALU by PCR indicated a similar AST-OPC1 engraftment and migration profile as was observed histologically. At all assessed time points and in 62 of 64 assessed animals, the highest hALU levels were detected in the cervical spinal cord at the site of injury and AST-OPC1 administration. At 2 days post-treatment, AST-OPC1 cells were predominantly restricted to the cervical spinal cord, while some animals treated with high dose AST-OPC1 also exhibited low levels of human cells in the thoracic spinal cord and brainstem/pons (Supporting Information Fig. 1A). At 3 and 6 months post-treatment, the same rostral/caudal distribution was observed but with higher levels of hALU detected at these later time points, (Supporting Information Fig. 1B; Fig. 3C), further suggesting that the engrafted cells underwent a proliferative phase prior to 6 months. Consistent with prior studies [10], levels of hALU in blood and CSF remained below, and in a few cases right at, the lower limit of quantitation of the assay, indicating that little to no AST-OPC1 migration occurred outside the CNS parenchyma.

Toxicology of AST-OPC1 in the Nude Rat Cervical SCI Model

To further assess the safety of AST-OPC1 treatment in cervical SCI, we conducted two cGLP toxicology studies designed to identify any toxicities associated with AST-OPC1 and with respect to (a) direct administration into the injured cervical spinal cord, (b) impact on organ function, (c) potential for induction of allodynia, and (d) capacity for tumor or ectopic tissue formation. Using the

same injury and transplant parameters as the above biodistribution studies, adult female nude rats were then examined clinically for 9 months post-treatment, followed by a full necropsy and histological examination of spinal cord and brain by an independent board-certified veterinary pathologist. A complete list of the in-life and post-mortem endpoints is shown in Supporting Information Table 2. Across the two studies, three different lots of clinical grade AST-OPC1 (manufactured by current Good Manufacturing Practices, cGMP) were assessed relative to injured rats treated with HBSS ($N = 31$), with one AST-OPC1 lot tested at both the efficacy dose (2.4×10^5 cells per rat, $N = 50$) and the maximum feasible dose (2.4×10^6 cells per rat, $N = 58$) and two lots tested at the maximum feasible dose only (AST-OPC1 Lot A, $N = 62$, AST-OPC1 Lot B, $N = 67$).

Based on the in-life clinical observations from both toxicology studies, no adverse side effects were associated with AST-OPC1 administration up to 9 months post-treatment. No significant differences were observed in body weights or any of the clinical assessments, including behavioral activity, excretion, external appearance, or skin conditions. Chronic neuropathic pain is a debilitating condition that occurs in approximately half of all SCI patients [27]. To identify any long-term changes in pain signaling potentially associated with AST-OPC1, animals were assessed for allodynia at 4 and 8 months post-SCI. Consistent with preclinical safety testing of AST-OPC1 in thoracic SCI [10], no differences were observed between AST-OPC1- and vehicle-treated animals in response to non-noxious thermal stimuli (Supporting Information Fig. 2).

Mortality rates were similar across treatment groups, with 21 of 31 vehicle-treated animals (68%) and 188 of 237 total AST-OPC1-treated animals (79%) surviving until the 9 month termination time point. Most commonly, mortality in all groups was a result of septicemia/inflammation or urogenital dysfunction, likely reflecting both the immunocompromised state of the animals and the expected pathophysiology after cervical SCI. Prior to the scheduled necropsy, clinical pathology evaluations were conducted on all animals and indicated no significant differences between the vehicle and AST-OPC1 treatment groups (see Supporting Information Table 2 for list of pathology measures).

Following terminal necropsy, histological examination of spinal cord and brain tissues was conducted to identify any microscopic changes within the CNS, including any potential teratoma or ectopic tissue formation associated with AST-OPC1. At 9 months post-treatment, large areas of cavitation and myelin loss were observed in HBSS-treated animals (Fig. 4A). In contrast, the injury site of AST-OPC1-treated animals typically remained intact and contained myelinated axons (Fig. 4B, 4C). In addition, large numbers of surviving AST-OPC1 cells were observed within the injury site at 9 months (Fig. 4D, 4F), with few cells exhibiting positive labeling with the proliferation marker Ki67 (Fig. 4E, 4G). Across both toxicology studies, AST-OPC1 engraftment in the cervical spinal cord was confirmed in 235 of 237 (99%) rats that were treated with AST-OPC1 and assessed for hALU labeling by ISH. Further, quantification of the maximal lesion area indicated a reduction in lesion area was associated with AST-OPC1, with most AST-OPC1-treated animals exhibiting no cavitation at the injury site (Fig. 4H).

To identify any microscopic pathologies associated with AST-OPC1 in the CNS, spinal cord and brain tissue sections were examined by an independent board certified veterinary pathologist. For these analyses, over 50 tissue sections were examined for each animal that included the entire length of the spinal cord and 5

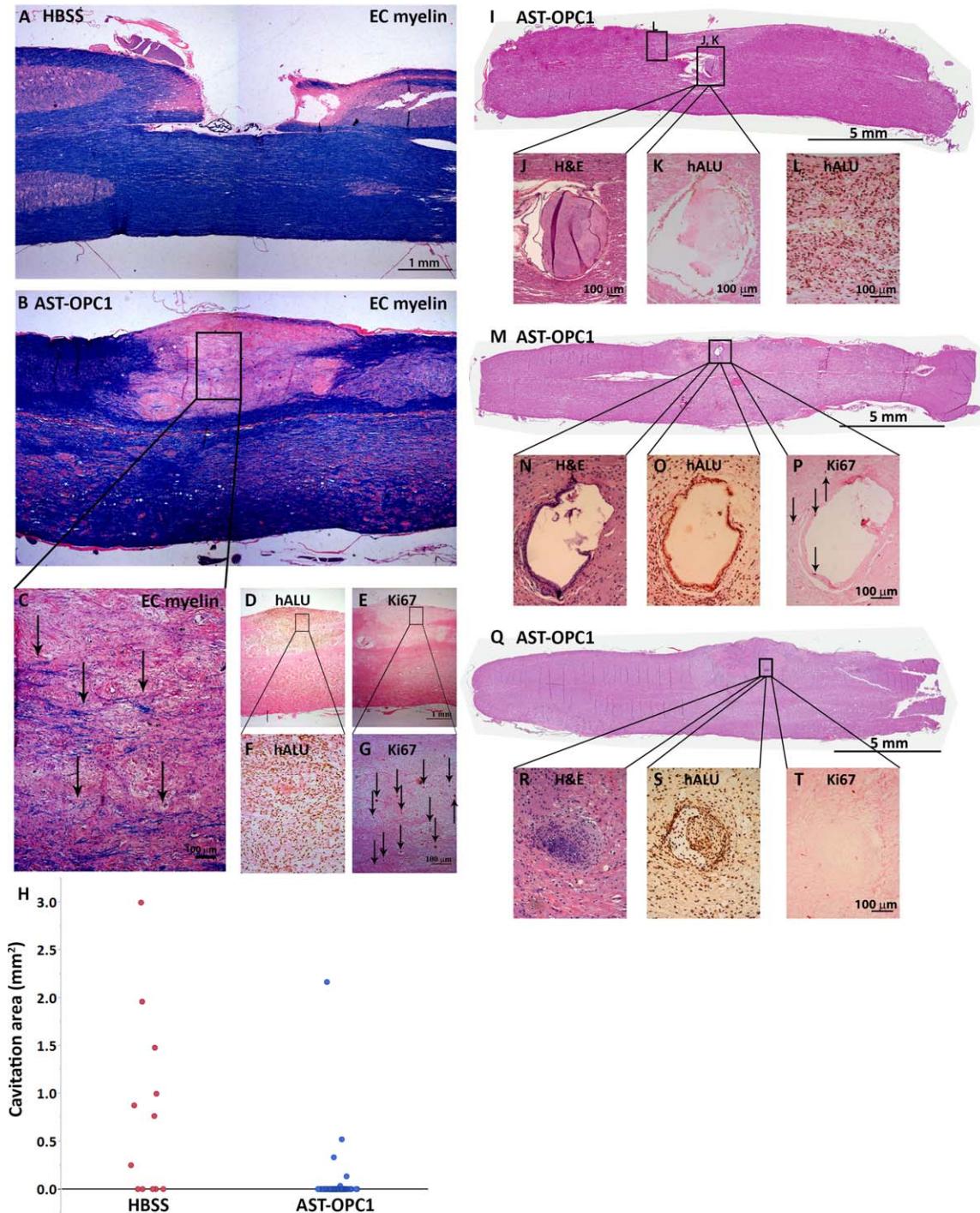


Figure 4. Safety/toxicological findings associated with AST-OPC1 administration after cervical SCI. **(A–C):** Representative photomicrographs of the cervical spinal cord injury site in HBSS (A) and AST-OPC1 (B, C) treated rats at 9 months post-treatment and stained with EC and eosin. The black box in (B) indicates the region depicted at higher magnification in panel (C) in which black arrows indicate examples of EC-labeled myelinated axons. **(D–G):** in situ hybridization - or immunohistochemistry-based labeling with hALU (D, F) or Ki67 (E, G) of the injury/graft site of an AST-OPC1-treated rat within the same region that myelinated host axons were observed. Black boxes in (D, E) indicate the magnified regions in (F, G). Black arrows in (G) indicate representative cells with positive Ki67 labeling. **(H):** Dot plot of parenchymal cavitation area for rats treated with HBSS (red dots) or AST-OPC1 (blue dots). **(I–L):** A non-human-derived epithelial-like cystic structure observed within the injury site of an AST-OPC1-treated rat stained with H&E (I, J) and confirmed to be of non-human origin given an absence of labeling with hALU (K). Cells positive for hALU are visible within the adjacent graft tissue but are not associated with the ectopic structure (L). **(M–T):** A human-derived epithelial-like cystic structure (M–P) and cartilage structure (Q–T) within the injury site of two different AST-OPC1-treated rats. Both ectopic structures were stained with H&E (M, N, Q, R), confirmed to be of human origin by positive labeling with hALU (O, S), and exhibiting minimal labeling with Ki67 (P, T). Black arrows in (P) indicate cells with positive labeling for Ki67. Abbreviations: EC, eriochrome cyanine; H&E, hematoxylin and eosin; HBSS, Hanks’ balanced salt solution; hALU, human ALU.

Table 1. Summary of ectopic tissues observed in AST-OPC1 preclinical toxicology studies in cervical SCI

Species origin ^a	Tissue type	Frequency ^b	Avg. max. diameter (μm) ^c	Rel. amount of Ki67+ cells ^d
Rat	Keratin cyst	2% (6/268)	788	Minimal
Rat	Epithelial cyst	0.4% (1/268)	942	Minimal
Human	Epithelial cyst	0.8% (2/237)	384	Minimal
Human	Cartilage	3% (8/237)	293	Minimal

^aSpecies of origin was determined based on labeling with human Alu DNA repeat sequence probe (hALU) by in situ hybridization. Ectopic structures that were positive for hALU were determined to be of human origin, whereas ectopic structures that were negative for hALU were determined to be of non-human origin (i.e., rat).

^bFrequency was calculated as the number of animals exhibiting each origin/type of ectopic structure out of the total number of assessed animals. Vehicle-treated animals were excluded when calculating the frequency of human origin ectopic structures.

^cAverage maximum diameter was calculated as the mean long axis diameter for all observed ectopic structures of a given origin/type.

^dRelative amount of Ki67-positive cells was scored as minimal if fewer than five labeled cells were detected within a single stained tissue section.

levels of the brain (medulla/pons, cerebellum, midbrain, forebrain and olfactory bulb). A teratoma was defined as an expansile proliferation or mass containing cells derived from at least two different germ layers (endodermal, mesodermal, or ectodermal). Out of 31 HBSS-treated animals and 237 AST-OPC1-treated animals, no teratomas or mineralization were observed in the spinal cord or brain of any animal, consistent with prior safety testing of AST-OPC1 in thoracic SCI [10].

Previously, a low frequency of microscopic ectopic tissue formation within the injury/graft site was observed during preclinical testing of AST-OPC1 in thoracic SCI [10], and thus also was assessed in the cervical toxicology studies. Similar to the findings in thoracic SCI, a low frequency of microscopic ectopic tissue formation was observed in both cervical toxicology studies and in both HBSS- and AST-OPC1-treated animals. For each identified ectopic structure, the presence of hALU was assessed by ISH, and ectopic structures found to contain human cells were assessed for Ki67 positivity by IHC.

Rat-derived ectopic structures (negative for hALU) were identified in a subset of HBSS- and AST-OPC1-treated rats and were observed within the cervical and thoracic spinal cord. One such ectopic structure was identified as an epithelial-like cyst (Fig. 4I, 4J) of rat origin based on negative labeling for hALU (Fig. 4K), adjacent to the injury/graft site of an AST-OPC1-treated rat (hALU positive cells within the nearby graft are shown in Fig. 4L). The remaining rat-derived structures were identified as keratin cysts and similarly were confirmed to be of rat origin based on negative labeling for hALU (Supporting Information Fig. 3). Rat-derived structures were observed at similar frequencies in vehicle and AST-OPC1-treated rats (vehicle: 3%, 1/31; AST-OPC1: 3%, 6/237).

Human-derived ectopic structures (identified as hALU positive) were identified in a subset of AST-OPC1-treated animals either within or immediately adjacent to the injury/graft site. Human-derived ectopic structures were either epithelial-like cysts, similar to the rat ectopic structure described above, or cartilage (Fig. 4M–4T). Both types of human-derived ectopic structures contained very few proliferative cells based on minimal labeling with Ki67 (Fig. 4P, 4T), and typically were smaller than rat-derived ectopic structures based on measurements of their long axis diameter (Supporting Information Table 3). Further, while a single epithelial-like cyst was observed in one low dose and one high dose AST-OPC1-treated rat, cartilage was only observed in subjects treated with high dose AST-OPC1 (2.4×10^6 cells per rat). The overall frequencies of rat and human ectopic tissue formation was similar (rat-derived structures = 2.6%, 7 of 268 HBSS- and AST-OPC1-treated rats; human-derived structures = 4.6%, 11 of 237

AST-OPC1-treated rats). With respect to the safety parameters assessed in this study (Supporting Information Table 2) and over the course of the 9 month observation period, no adverse clinical signs were associated with any of the observed ectopic structures, regardless of the species of origin. A summary of the ectopic tissue formation identified in the toxicology studies is shown in Table 1. A summary of all the in vivo studies, including their design, endpoints and key findings is shown in Table 2.

DISCUSSION

To advance the clinical testing of AST-OPC1 from thoracic to cervical SCI, a series of preclinical efficacy and safety studies were conducted and submitted to the U.S. FDA as part of an IND amendment for AST-OPC1. Findings from these studies expand the overall efficacy and safety profile associated with AST-OPC1 and suggest the type of preclinical testing that should be considered for candidate cell therapies in development for SCI and other forms of CNS injury and disease.

Previously, efficacy of AST-OPC1 was demonstrated in rat models of thoracic SCI and cervical SCI, where motor behavioral recovery was measured using the Basso, Beattie, Bresnahan Locomotor Rating Scale, and three or four-parameter kinematic analyses [11, 12, 28]. The results presented here independently confirmed the efficacy of AST-OPC1 in a different rat model of cervical SCI (unilateral contusion in nude rats as opposed to prior testing with bilateral midline contusion in Sprague Dawley rats) and were based on automated analysis of 90 distinct gait parameters using the TreadScan system. By combining all 90 gait parameters in a PCA, we obtained an unbiased readout of overall gait performance, which was then used to identify individual gait parameters, such as running speed and longitudinal deviation of the ipsilateral forelimb that exhibited the greatest AST-OPC1-associated improvements. While prior observations of AST-OPC1 efficacy were followed for 2 months post-treatment [12], our findings extend the AST-OPC1 associated improvements up to 4 months post-treatment. In addition, it is important to note that while AST-OPC1-associated improvements resulted in an intermediate level of locomotor performance when compared to uninjured (sham) animals, the specific improvements in forelimb motor function are encouraging given that even partial restoration of arm and hand function can have a big impact on the quality of life of cervical SCI patients [5].

While the potential safety concerns associated with advancing AST-OPC1 treatment from thoracic to cervical SCI were largely the

Table 2. Summary of AST-OPC1 preclinical studies in cervical SCI

Study type, cGLP/non-cGLP	Species, model and delivery route	Study duration	Treatment groups (n)	No. of AST-OPC1 lots	Study endpoints	Key findings
Efficacy Study, non-cGLP	Adult athymic nude rat, cervical SCI, ISC	4 months	Sham (8) Vehicle (16) AST-OPC1, L (16)	1	<ul style="list-style-type: none"> Functional recovery using TreadScan system Histological analyses of spinal cord 	<ul style="list-style-type: none"> AST-OPC1 enhanced recovery of locomotor performance after cervical SCI relative to Vehicle AST-OPC1 cells persisted at the injury site and reduced parenchymal cavitation at 4 months
Biodistribution Study 1, cGLP	Adult athymic nude rat, cervical SCI, ISC	2 days, 3, 6, 9 months	2 days V (10), L (10), H (10) 3 months V (10), L (13), H (18) 6 months V (9), L (13), H (19) 9 months V (5), L (9), H (20)	2	<ul style="list-style-type: none"> Mortality/morbidity Clinical observations Histological examination of spinal cord and brain, including detection of human cells by hALU 	<ul style="list-style-type: none"> No significant differences in any in-life endpoints Human cells detected in cervical spinal cord at all time points in 111 of 112 rats Most rostral AST-OPC1 migration observed in brainstem, caudal to pontine nucleus Most caudal AST-OPC1 migration observed in thoracic spinal cord at T1-T2 (high dose only)
Biodistribution Study 2, cGLP	Adult athymic nude rat, cervical SCI, ISC	2 days, 3, 6 months	2 days V (10), L (10), H (10) 3 months V (11), L (11), H (11) 6 months V (11), L (11), H (11)	1	<ul style="list-style-type: none"> Quantitation of hALU in spinal cord, brain, CSF, and blood by real-time PCR 	<ul style="list-style-type: none"> AST-OPC1 engraftment frequency and migration profile consistent with Biodistribution Study 1 Increasing numbers of human cells detected in cervical spinal cord at later time points Little or no (below quantifiable levels) of hALU detected in other brain regions, CSF, and blood
Toxicology Study 1, cGLP	Adult athymic nude rat, cervical SCI, ISC	9 months	Vehicle (19) AST-OPC1, L (50) AST-OPC1, H (58)	1	<ul style="list-style-type: none"> Mortality/morbidity Clinical observations Allodynia Clinical pathology (organ weights, hematology & clinical chemistries) Histological examination of spinal cord and brain 	<ul style="list-style-type: none"> No AST-OPC1-related effects on in-life or clinical pathology assessments AST-OPC1 engraftment observed in >98% of rats at 9 months post-transplant No tumor or teratoma formation observed Very low freq. of asymptomatic human and non-human (rat) ectopic tissue formation observed within injury/graft site (1 human epithelial-like cyst) Little to no proliferative capacity (Ki67 positivity) observed within AST-OPC1 graft and ectopic structures
Toxicology, Study 2, non-cGLP	Adult athymic nude rat, cervical SCI, ISC	9 months	Vehicle (12) AST-OPC1 Lot A, H (62) AST-OPC1 Lot B, L, (67)	2	<ul style="list-style-type: none"> Same endpoints as Toxicology Study 1, except no allodynia testing performed 	<ul style="list-style-type: none"> Same findings as Tox. Study 1, except low freq. of human ectopic tissue formation also included microscopic cartilaginous structures that were asymptomatic and non-proliferative at 9 months

Abbreviations: cGLP, current good laboratory practices; CSF, cerebral spinal fluid; hALU, human Alu DNA repeat sequence probe; H, high dose AST-OPC1 (2.4×10^6 cells per rat); ISC, intraspinal cord; L, low dose AST-OPC1 (2.4×10^5 cells per rat); V, vehicle.

same, one remaining question was whether delivery of AST-OPC1 into the cervical spinal cord could increase the likelihood of transplanted cells migrating into the brain. To address this, we conducted large scale biodistribution studies in nude rats with cervical SCI and tracked AST-OPC1 migration visually by histology and quantitatively by real-time PCR. Both of these approaches indicated that AST-OPC1 cells could reach the rat brainstem when delivered at a maximum feasible dose (2.4×10^6 cells per rat), with a small number of these cells also migrating as rostral as the medulla/pons. In contrast, when a lower dose of AST-OPC1 (2.4×10^5 cells per rat) was administered, rostral migration was limited to the high cervical spinal cord. Importantly, this lower AST-OPC1 dose is proportional to the highest proposed clinical doses of AST-OPC1 (1×10^7 to 2×10^7 cells per patient) based on $50\times$ volumetric scaling of the rat and human spinal cord [29]. Further, given an observed parenchymal migration of approximately 3 cm, AST-OPC1 cells administered into the human cervical spinal cord would be expected to extend a maximum of 2 segments from the graft site, based on an average cervical segment length of approximately 1.5 cm [30]. Given the substantially longer distance required to migrate through the human spinal cord, and that the administration procedure did not cause cell dissemination into the CSF or blood, it is not expected that AST-OPC1 migration would reach the human brain.

As an embryonic stem cell-derived product, possibly the greatest theoretical concern associated with AST-OPC1 is its potential to form teratomas, tumors, or expansive ectopic structures that might result from residual undifferentiated cells or other progenitor cells present in the transplanted population. Similar to the safety testing conducted for thoracic SCI, identification of such structures was a key endpoint of the cervical toxicology studies, which were thus designed to test a large number of animals receiving up to the maximum feasible dose of AST-OPC1 and assessed up to 9 months post-transplant. Based on the combined results of the thoracic [10] and cervical toxicology studies, a total of 489 nude rats received a direct injection of AST-OPC1 into the injured spinal cord, and cumulatively, approximately 9.6×10^8 AST-OPC1 cells were assessed for safety in these toxicology studies. Across all these studies, no animals were found to develop teratomas or tumors following AST-OPC1 treatment.

Consistent with the thoracic safety studies that supported initiation of the AST-OPC1 thoracic SCI clinical trial [10], rare occurrences of asymptomatic epithelial-like cystic structures were observed in the cervical toxicology studies reported here. Of note, these findings also included detection of endogenous non-human cystic structures in AST-OPC1- and vehicle-treated rats, suggesting that similar ectopic tissue formation may be a natural, albeit infrequent, component of this injury model, potentially as a result of post-injury tissue remodeling and similar to what is seen in human SCI [3]. In 2 out of 267 AST-OPC1-treated rats, formation of a single human-derived epithelial-like cystic structure was observed within the injury/graft site. Importantly, these findings contrast a 2008 preclinical study conducted by Geron Corporation that detected human-derived epithelial-like cysts at a much higher frequency and resulted in a clinical hold. To address this, Geron conducted additional preclinical studies that identified the contaminating epithelial progenitor cell as well as associated epithelial cell markers that could be used to detect this type of cellular impurity in AST-OPC1. Upon demonstrating that additional candidate clinical lots of AST-OPC1 contained minimal levels of contaminating epithelial cells and exhibited minimal capacity for

ectopic cyst formation in vivo [10], the clinical hold was removed, and in 2010, the thoracic trial was initiated.

For the cervical toxicology studies reported here, ectopic structures associated with AST-OPC1 also included rare instances of ectopic cartilage formation, observed with the maximum feasible AST-OPC1 dose only. In the case of the maximum feasible dose (2.4×10^6 cells per rat), administration of this high cell number into a constrained space (i.e., spinal cord parenchyma) may have resulted in cell compaction, a known step in the process of chondrogenesis [31]. To minimize the possibility of this during clinical testing, the highest planned clinical dose of AST-OPC1 at 2×10^7 per patient is approximately $6\times$ lower and will use a $12\times$ lower injection volume than the maximum feasible dose used in these preclinical studies (based on a $50\times$ volumetric conversion factor [29]). Nonetheless, identification and elimination of ectopic tissue-forming cells remains a critical focus for the continued development of AST-OPC1 and other stem cell or progenitor-based cell therapies. Detection of cartilaginous ectopic structures suggests that low levels of mesenchymal progenitors [32], or epithelial progenitors able to undergo epithelial to mesenchymal transition [33] may arise during the AST-OPC1 differentiation process (with the latter cell type potentially explaining both types of observed ectopic tissue) and, therefore, require appropriate screening assays and depletion methods to detect and eliminate these cells.

A major challenge for screening assays is the need to detect ectopic tissue-forming cells at an extremely low frequency, well beyond the capacity of conventional marker screening. In the case of AST-OPC1, ectopic structures remained small with little to no proliferative capacity after 9 months, suggesting that each structure could represent a clonal or near clonal event. Based on this hypothesis, the frequency of cartilage-forming cells in AST-OPC1 is approximately $1/5.6 \times 10^7$ or 0.000018% (calculation based on maximum feasible dose transplants only). While advancements in single cell profiling may ultimately allow reliable detection at such a low frequency, recent efforts at Asterias have instead focused on the development of in vitro model systems that can amplify and detect the rare ectopic tissue-forming cells. By using these impurity bioassays, in conjunction with modifications to the AST-OPC1 production process that further restricts cells to the neural/glial lineage, it is expected that even the low level capacity of ectopic tissue formation will be eliminated from this cell therapy product. A manuscript describing such impurity bioassays and modifications to the AST-OPC1 production process is currently in preparation.

While some inherent risks remain for stem cell-based therapies such as AST-OPC1, these concerns must be weighed against the potential therapeutic benefit. In the case of AST-OPC1, significant improvements in motor behavioral recovery have been observed in thoracic SCI models [11] and in cervical SCI models by independent labs (this manuscript and [12]), and prior studies have indicated multiple mechanisms potentially contribute to AST-OPC1's therapeutic activity, including robust engraftment and migration within the spinal cord, suppression of parenchymal cavitation, secretion of trophic factors [9], support of myelinated axons within the injury site, and maturation into myelin producing oligodendrocytes [6, 10]. These in vivo actions have been linked to other stem cell-based therapies in development for SCI, including neural stem cells (NSCs, [34–37]), mesenchymal stem cells (MSCs, [38, 39]), and other OPCs [40–44]; however, only a few of these approaches have advanced to the clinic. Of the other clinical stage stem cell-based therapies for SCI, autologous MSCs have been tested in five trials [45], two preparations of fetal-derived NSCs have been tested [46, 47], and AST-OPC1 remains the only OPC-

based approach tested to date. Because AST-OPC1 has the capacity to act via all of the above therapeutic mechanisms and exhibited an acceptable preclinical safety profile, it is potentially well suited to address the complex milieu of cellular events that give rise to tissue damage and impairment after SCI.

Going forward, there are remaining questions about AST-OPC1's therapeutic activity that will need to be addressed to help guide clinical development, including whether AST-OPC1 can impact recruitment or maturation of endogenous OPCs, whether there are differences in the short- versus long-term effects on the host microenvironment following AST-OPC1 treatment, and perhaps most importantly, which of these and the previously published actions of AST-OPC1 drive the observed improvements in motor behavior recovery. In addition, it will be important for future studies to incorporate electrophysiological monitoring to determine if the improvements in motor behavior recovery are correlated with any changes in host neuronal function. A deeper understanding of how these different mechanisms relate to AST-OPC1's therapeutic activity may ultimately reveal mechanistic endpoints to monitor in future clinical trials and can help guide development of candidate potency assays for AST-OPC1 and other cell therapies. In future studies, it also will be important to compare AST-OPC1 to other candidate cell therapies and additional transplant controls, such as heat-killed cells, to better understand the extent to which the engrafted AST-OPC1 cells can directly influence their host environment and whether multiple cell types improve injury outcome via distinct or common pathways.

Disclosure of preclinical efficacy and safety studies for candidate cell therapy products is important because such studies can inform the design of clinical testing and help guide preclinical development of future cell therapy products. For AST-OPC1, the results presented here guided subsequent clinical testing in multiple ways. First, the highest planned clinical dose of AST-OPC1 (2×10^7 cells/patient) and clinical administration method (direct intraspinal administration) were designed to match the preclinical dosing strategy (2.4×10^5 cells per rat, intraspinal) that was both efficacious and exhibited a favorable safety profile with no migration into the brain or formation of ectopic cartilage. Second, the decision to target the sub-acute phase of cervical SCI in the clinical trial was supported by AST-OPC1 administration at 1 week post-injury in rats. While it is difficult to understand the precise temporal relationship for SCI progression in rodents versus humans, studies have indicated potential links between the plateau in spontaneous recovery, resolution of cavitation and glial scar formation within the injury site, and transition from the subacute to chronic phase post-SCI [22, 26, 48]. In the case of rats, spontaneous recovery and cavitation/glial scar formation typically resolves within 4 weeks post-SCI [22, 24–26], whereas these processes may persist for 4–6 months in patients with sensorimotor complete cervical SCI [48]. Conservatively equating 1 week post-injury in rats to 1 month in humans, the initial design of the cervical clinical trial included a dosing window of up to 30 days post-injury.

Similarly, findings from the preclinical biodistribution and toxicology studies informed decisions regarding post-treatment monitoring of enrolled patients. For example, the confirmed absence of AST-OPC1 cells in CSF or blood indicated that safety monitoring should be focused on the CNS. Second the ability of AST-OPC1 to suppress parenchymal cavitation supported continued monitoring of the patients' injury site by MRI. Going forward, future cell therapies must consider what degree of preclinical efficacy and safety testing is needed prior to clinical translation. Similar to AST-OPC1, stem cell-based therapies must include large scale biodistribution and toxicology studies to determine if parameters such as

cell migration, proliferation, tumor formation, or differentiation into unintended cell types pose any significant safety concerns, and alternatively, whether any potentially beneficial physiological or anatomical changes associated with the treatment might allow for non-invasive monitoring during clinical testing.

Collectively, results of the studies presented here in conjunction with prior publications supported initiation of a phase I/IIa dose escalation clinical trial testing AST-OPC1 in patients with cervical SCI. The initial trial design included treatment of up to 13 patients with AST-OPC1 doses ranging from 2 to 20 million cells (3–5 patients per dose cohort) and has since been expanded to include treatment of up to 35 patients with sub-acute, C5 to C7, motor complete (AIS-A or AIS-B) cervical SCI. Long-term safety and efficacy monitoring will be conducted up to 15 years.

CONCLUSION

To support the clinical use of the OPC therapy, AST-OPC1, for cervical SCI, we report the results of a series of preclinical efficacy and safety studies. Nude rats subjected to cervical SCI and treated with AST-OPC1 exhibited enhanced motor behavioral recovery as measured by improvements in locomotor performance relative to vehicle controls using the automated TreadScan system. Enhanced motor behavioral recovery was observed up to 4 months post-treatment and was associated with robust AST-OPC1 engraftment, migration into the lesion site, and suppression of parenchymal cavitation. AST-OPC1 biodistribution following direct administration into the injured cervical spinal cord was limited to the spinal cord and lower brainstem, while remaining minimal or absent from the CSF and blood. No significant toxicities were associated with AST-OPC1 treatment after cervical SCI, including no impacts on mortality, morbidity, development of allodynia, and no detected instances of teratoma or tumor formation. These results supported initiation of a phase I/IIa clinical trial in the U.S. for patients with sensorimotor complete cervical SCI and provide an example of the extent of preclinical testing that should be considered for similar cell therapy products in development for CNS injury and disease.

ACKNOWLEDGMENTS

We thank the following individuals for their contributions: Elham Yeganeh and manufacturing colleagues for cGMP production of AST-OPC1, Karen Delavan-Boorsma, Stacy Kanno, and Samantha Edel for performing rodent surgical procedures and providing animal husbandry support, Amanda Conta and Simona Neumann for performing rodent surgical procedures and TreadScan method development/data acquisition, Yelena Polonskaya for performing histological analyses, Rachel Tapp for directing biodistribution and toxicology studies at MPI Research, and Casey Case for consultation on manuscript preparation. All work described in this manuscript was funded by Geron Corporation and Asterias Biotherapeutics, Inc. C.A.P. is currently affiliated with Neurona Therapeutics, South San Francisco, CA; J.D. is currently affiliated with Dark Horse Consulting, Campbell, CA.

AUTHOR CONTRIBUTIONS

N.C.M.: collection of data, data analysis and interpretation, manuscript writing; C.A.P.: Conception and design, collection of data, data analysis and interpretation, final approval of manuscript; J.D.: Conception and design, data analysis and interpretation, final

approval of manuscript; E.D.W. and J.S.L.: Conception and design, data interpretation, final approval of manuscript.

DISCLOSURE OF POTENTIAL CONFLICTS OF INTEREST

C.A.P., J.D., E.D.W., and J.S.L. were employees of Geron Corporation when the studies were conducted. N.C.M., E.D.W., and

J.S.L. are employed by Asterias Biotherapeutics, Inc. In the U.S. and internationally, patents have been filed and issued for AST-OPC1. The authors have no other relevant affiliations or financial involvement with any organizations or entities with a potential conflict of interest with any of the subject matter in this manuscript apart from those disclosed.

REFERENCES

- Kakulas BA. The applied neuropathology of human spinal cord injury. *Spinal Cord* 1999; 37:79–88.
- Anderson DK, Hall ED. Pathophysiology of spinal cord trauma. *Ann Emerg Med* 1993; 22:987–992.
- Norenberg MD, Smith J, Marcillo A. The pathology of human spinal cord injury: Defining the problems. *J Neurotrauma* 2004;21: 429–440.
- Almad A, Sahinkaya FR, McTigue DM. Oligodendrocyte fate after spinal cord injury. *Neurotherapeutics* 2011;8:262–273.
- Anderson KD, Fridén J, Lieber RL. Acceptable benefits and risks associated with surgically improving arm function in individuals living with cervical spinal cord injury. *Spinal Cord* 2009;47:334–338.
- Nistor GI, Totoiu MO, Haque N et al. Human embryonic stem cells differentiate into oligodendrocytes in high purity and myelinate after spinal cord transplantation. *Glia* 2005;49: 385–396.
- Hu BY, Du ZW, Zhang SC. Differentiation of human oligodendrocytes from pluripotent stem cells. *Nat Protoc* 2009;4:1614–1622.
- Alsanie WF, Niclis JC, Petratos S. Human embryonic stem cell-derived oligodendrocytes: Protocols and perspectives. *Stem Cells Dev* 2013;22:2459–2476.
- Zhang YW, Denham J, Thies RS. Oligodendrocyte progenitor cells derived from human embryonic stem cells express neurotrophic factors. *Stem Cells Dev* 2006;15:943–952.
- Priest CA, Manley NC, Denham J et al. Preclinical safety of human embryonic stem cell-derived oligodendrocyte progenitors supporting clinical trials in spinal cord injury. *Regen Med* 2015;10:939–958.
- Keirstead HS, Nistor G, Bernal G et al. Human embryonic stem cell-derived oligodendrocyte progenitor cell transplants remyelinate and restore locomotion after spinal cord injury. *J Neurosci* 2005;25:4694–4705.
- Sharp J, Frame J, Siegenthaler M et al. Human embryonic stem cell-derived oligodendrocyte progenitor cell transplants improve recovery after cervical spinal cord injury. *STEM CELLS* 2010;28:152–163.
- Muramoto A, Imagama S, Natori T et al. Midkine overcomes neurite outgrowth inhibition of chondroitin sulfate proteoglycan without glial activation and promotes functional recovery after spinal cord injury. *Neurosci Lett* 2013;550:150–155.
- Gensel JC, Tovar CA, Hamers FP et al. Behavioral and histological characterization of unilateral cervical spinal cord contusion injury in rats. *J Neurotrauma* 2006;23:36–54.
- Lee JH, Streijger F, Tigchelaar S et al. A contusive model of unilateral cervical spinal cord injury using the infinite horizon impactor. *J Vis Exp* 2012;24:pii: 3313.
- Hosier H, Peterson D, Tsymalyuk O et al. A Direct comparison of three clinically relevant treatments in a rat model of cervical spinal cord injury. *J Neurotrauma* 2015;32: 1633–1644.
- Walker CL, Wang X, Bullis C et al. Biphasic bisperoxovanadium administration and Schwann cell transplantation for repair after cervical contusive spinal cord injury. *Exp Neurol* 2015;264:163–172.
- Geissler SA, Schmidt CE, Schallert T. Rodent models and behavioral outcomes of cervical spinal cord injury. *J Spine* 2013;(suppl 4):001.
- Lebkowski J, Fessler R, Chen D et al. Clinical Assessment of hESC-Derived Oligodendrocyte Progenitor Cells (AST-OPC1) in Patients with Sensorimotor-Complete Thoracic and Cervical Spinal Cord Injuries. International Society for Stem Cell Research, San Francisco, CA, 2016.
- Xu C, Inokuma MS, Denham J et al. Feeder-free growth of undifferentiated human embryonic stem cells. *Nat Biotechnol* 2001;19: 971–974.
- Li Y, Powell S, Brunette E et al. Expansion of human embryonic stem cells in defined serum-free medium devoid of animal-derived products. *Biotechnol Bioeng* 2005;91:688–698.
- Scheff SW, Rabchevsky AG, Fugaccia I et al. Experimental modeling of spinal cord injury: Characterization of a force-defined injury device. *J Neurotrauma* 2003;20:179–193.
- Hulsebosch CE, Xu GY, Perez-Polo JR et al. Rodent model of chronic central pain after spinal cord contusion injury and effects of gabapentin. *J Neurotrauma* 2000;17:1205–1217.
- Ek CJ, Habgood MD, Callaway JK et al. Spatio-temporal progression of grey and white matter damage following contusion injury in rat spinal cord. *PLoS One* 2010;5:e12021.
- Hu R, Zhou J, Luo C et al. Glial scar and neuroregeneration: Histological, functional, and magnetic resonance imaging analysis in chronic spinal cord injury. *J Neurosurg Spine* 2010;13:169–180.
- Patel SP, Smith TD, VanRooyen JL et al. Serial diffusion tensor imaging in vivo predicts long-term functional recovery and histopathology in rats following different severities of spinal cord injury. *J Neurotrauma* 2016;33: 917–928.
- Baastrup C, Finnerup NB. Pain in spinal cord injury. *Pain Manag* 2012;2:87–94.
- Basso DM, Beattie MS, Bresnahan JC. A sensitive and reliable locomotor rating scale for open field testing in rats. *J Neurotrauma* 1995;12:1–21.
- Metz GA, Curt A, van de Meent H et al. Validation of the weight-drop contusion model in rats: A comparative study of human spinal cord injury. *J Neurotrauma* 2000;17:1–17.
- Ko HY, Park JH, Shin YB et al. Gross quantitative measurements of spinal cord segments in human. *Spinal Cord* 2004;42:35–40.
- Raghothaman D, Leong MF, Lim TC et al. Engineering cell matrix interactions in assembled polyelectrolyte fiber hydrogels for mesenchymal stem cell chondrogenesis. *Bio-materials* 2014;35:2607–2616.
- Huselstein C, Li Y, He X. Mesenchymal stem cells for cartilage engineering. *Biomed Mater Eng* 2012;22:69–80.
- Boyd NL, Robbins KR, Dhara SK et al. Human embryonic stem cell-derived mesoderm-like epithelium transitions to mesenchymal progenitor cells. *Tissue Eng Part A* 2009; 15:1897–1907.
- Cummings BJ, Uchida N, Tamaki SJ et al. Human neural stem cells differentiate and promote locomotor recovery in spinal cord-injured mice. *Proc Natl Acad Sci USA* 2005; 102:14069–14074.
- Karimi-Abdolrezaee S, Eftekharpour E, Wang J et al. Delayed transplantation of adult neural precursor cells promotes remyelination and functional neurological recovery after spinal cord injury. *J Neurosci* 2006;26:3377–3389.
- Perrin FE, Boniface G, Serguera C et al. Grafted human embryonic progenitors expressing neurogenin-2 stimulate axonal sprouting and improve motor recovery after severe spinal cord injury. *PLoS One* 2010;5: e15914.
- Kadoya K, Lu P, Nguyen K et al. Spinal cord reconstitution with homologous neural grafts enables robust corticospinal regeneration. *Nat Med* 2016;22:479–487.
- Osaka M, Honmou O, Murakami T et al. Intravenous administration of mesenchymal stem cells derived from bone marrow after contusive spinal cord injury improves functional outcome. *Brain Res* 2010;1343:226–235.
- Quertainmont R, Cantinieaux D, Botman O et al. Mesenchymal stem cell graft improves recovery after spinal cord injury in adult rats through neurotrophic and pro-angiogenic actions. *PLoS One* 2012;7:e39500.
- Wang S, Bates J, Li X et al. Human iPSC-derived oligodendrocyte progenitor cells can myelinate and rescue a mouse model of congenital hypomyelination. *Cell Stem Cell* 2013; 12:252–264.
- Yang N, Zuchero JB, Ahlenius H et al. Generation of oligodendroglial cells by direct lineage conversion. *Nat Biotechnol* 2013;31: 434–439.

42 Douvaras P, Wang J, Zimmer M et al. Efficient generation of myelinating oligodendrocytes from primary progressive multiple sclerosis patients by induced pluripotent stem cells. *Stem Cell Reports* 2014;3:250–259.

43 All AH, Gharibani P, Gupta S et al. Early intervention for spinal cord injury with human induced pluripotent stem cells oligodendrocyte progenitors. *PLoS One* 2015;10:e0116933.

44 Piao J, Major T, Auyeung G et al. Human embryonic stem cell-derived oligodendrocyte

progenitors remyelinate the brain and rescue behavioral deficits following radiation. *Cell Stem Cell* 2015;16:198–210.

45 Schroeder GD, Kepler CK, Vaccaro AR. The use of cell transplantation in spinal cord injuries. *J Am Acad Orthop Surg* 2016;24:266–275.

46 Shin JC, Kim KN, Yoo J et al. Clinical trial of human fetal brain-derived neural stem/progenitor cell transplantation in patients with traumatic cervical spinal cord injury. *Neural Plast* 2015;2015:630932.

47 Huhn S, Gage A, Kalsi-Ryan S et al. Motor and functional gains demonstrated in a dose-escalation arm of a phase II neural stem cell transplantation study in cervical spinal cord injury. International Society for Stem Cell Research, San Francisco, CA, 2016.

48 Fawcett JW, Curt A, Steeves JD et al. Guidelines for the conduct of clinical trials for spinal cord injury as developed by the ICCP panel: Spontaneous recovery after spinal cord injury and statistical power needed for therapeutic clinical trials. *Spinal Cord* 2007;45:190–205.



See www.StemCellsTM.com for supporting information available online.